JOURNAL OF AIRCRAFT
Vol. 32, No. 5, September–October 1995

Co- and Contrarotating Streamwise Vortices in a Turbulent Boundary Layer

Xin Zhang*
University of Southampton, Southampton SO17 1BJ, England, United Kingdom

A study was carried out on streamwise vortices in a turbulent boundary layer using computational fluid dynamics. The vortices were generated by either a single jet or an array of jets of co- or contrarotating arrangement exhausting into the boundary layer. The effects of jet angle, velocity ratio, and spacing were studied. Results confirmed previous experimental observations of single vortex formation at a sufficient distance downstream of the jet exit, from the initial multiple vortices. The study found that jet skew angle variation from 60 to 90 deg did not cause significant changes in the overall flow features. The results also suggested that a high jet velocity ratio might not necessarily be effective for flow control. For the contrarotating jets, it was found that 1) they produced stronger vortices, 2) the circulation level was reduced with the jet spacing, and 3) the maximum vorticity level was not affected by the jet spacing. For the corotating jets, it was found that 1) the circulation level was not affected by the jet spacing and 2) the vortices decayed much faster than those of the contrarotating arrangement. Good comparison was obtained between the calculated circulation levels and previous measurements.

Nomenclature

C_{fx} = streamwise skin friction coefficient
C_p = specific heat
D = jet diameter
D_s = jet spacing
k = turbulent kinetic energy
U, V, W = velocity components
V_j = jet exit velocity
V_∞ = cross-stream velocity
$\boldsymbol{V}$ = flow velocity in vector form
X, Y, Z = normalized coordinates, $X = x/D$, $Y = y/D$, and $Z = z/D$
x, y, z = Cartesian coordinates
α = jet pitch angle
Γ = cross-plane circulation, $-\int \bar{\Omega}_x \, dy \, dz$
δ = oncoming boundary-layer thickness
ε = turbulence dissipation rate
ζ = bulk viscosity
θ = jet skew angle
λ_j = jet velocity ratio, V_j/V_∞
μ = viscosity
ρ = density
σ_t = turbulent Prandtl number
τ = shear stress
$\bar{\Omega}_x$ = vorticity level on x plane, $(\delta/V_e)[(\partial W/\partial y) - (\partial V/\partial z)]$

I. Introduction

STREAMWISE vortices can be used to regulate a turbulent flow and separations through changes in the near-wall stress field. The vortices can be produced by small skewed and pitched jets exhausting into an oncoming flow. The interaction between the jet and the oncoming flow could produce embedded streamwise vortices, which have the ability of convecting kinetic and thermal energy in the cross plane. This ability could be utilized to control flow separation/stall,[1] to enhance film cooling efficiency of turbine blades,[2] and to promote heat transfer.[3,4] There are other application areas such as mixing promotion, secondary flow control, and lift enhancement.

In many applications, streamwise vortices are produced by small winglets.[1] They are cheap and effective devices. However, when submerged by local regions of separation and a thick boundary layer they are less effective. Winglets also induce drag penalties and hot spots. They could not be used for the purpose of active control. The idea of using jet-generated vortices was introduced by Wallis.[5] The so-called jet vortex generator (JVG) could overcome some of the limitations of the winglets. Since Wallis' experiment, applications of JVG have been limited. Apart from cost considerations, a lack of understanding and design guidelines contributed to their scarce use. Nevertheless, JVG has obvious merits. In the last few years, a number of studies were made on JVG. Freestone[6] tested geometrical effects of rectangular JVGs in a wind-tunnel experiment. Compton and Johnston[7] performed a wind-tunnel study of a single jet in a turbulent boundary layer. The film cooling process of 90-deg skewed corotating jets was described by Honami et al.[2] Apart from the experimental studies, a computational analysis of vortices was performed by Liandrat.[8] A single jet-induced fluid flow and heat transfer was analyzed by Zhang,[9] and Zhang and Collins,[4] and co- and contrarotating jets by Zhang.[3,9] Both k-ε and Reynolds stress models were employed. In Zhang,[3] the effect of the jet exit was studied and was found to have little effect on the downstream vortex development. At the same skew and pitch angles the dominant parameter was found to be the jet velocity ratio.

In this study, the induced flow of a single jet in a turbulent oncoming boundary layer is discussed first, which is followed by a discussion on the co- and contrarotating jets. The aim is to provide insight into the physics and to provide some design guidelines. The analysis was carried out using computational fluid dynamics (CFD). The mass-averaged Navier–Stokes equations were solved. Turbulence was modeled by a two-equation k-ε model and a differential Reynolds stress model.

II. Flow Conditions

In the previous studies,[3,4,9] the streamwise vortices generated by a single jet and their effects on both the fluid flow

Presented as Paper 93-3035 at the AIAA 24th Fluid Dynamics Conference, Orlando, FL, July 6–9, 1993; received July 25, 1993; revision received March 21, 1995; accepted for publication May 15, 1995.

*Lecturer, Department of Aeronautics and Astronautics. Member AIAA.

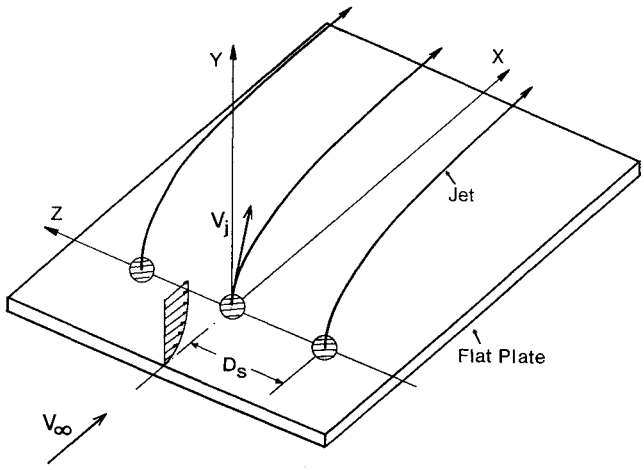

Fig. 1 Schematic of a corotating jet system.

and the heat transfer properties were addressed. λ_j and θ were varied to find the optimal parameters (in terms of vortex strength). Based on the single jet study, a jet pitched at α = 45 deg and skewed at θ = 60 deg was used in the current co- and contrarotating jet studies. The jet velocity and crossflow velocity ratio λ_j was fixed at 1.5. The spacing D_s between the two adjacent jet exit centers was varied. The results of the study were analyzed in terms of velocity, vorticity, and turbulent kinetic energy distributions. The development of the vortex was described in terms of circulation level, maximum vorticity, and skin friction, etc.

To produce the streamwise vortices, the jets were issued from a flat plate into an oncoming turbulent boundary layer (see Fig. 1). For the majority of the test cases the exit area of the jet was a circular one of 6.35 mm diameter. The cross section of the jet was, in fact, an ellipse. To validate the present numerical model and to compare the present results with the wind-tunnel data of Compton and Johnston,[7] a jet with a circular cross section of 6.35 mm diameter was used. For all the test cases, the velocity at the edge of the oncoming boundary layer was 15 m/s, and the Reynolds number based on the momentum thickness of the oncoming boundary layer was 1.5×10^3. The oncoming flow conditions were the same as those described in Compton and Johnston.[7]

In the current single jet study, the effects of λ_j were studied at α = 45 deg and θ = 45 deg. The values of λ_j were 0.25, 0.5, 0.7, 1.0, 1.5, 2.0, 2.5, and 3.0. The effects of the skew angle were studied at α = 45 deg and λ_j = 1.0. The values of θ were 0, 15, 30, 45, 60, 75, 90, 105, and 120 deg. For the co- and contrarotating JVG arrangements, α was fixed at 45 deg, θ at 60 deg, and λ_j at 1.5. The spacings between the two adjacent jet exit centers were $3D$, $5D$, $7D$ and $9D$.

III. Governing Equations

The governing equations used to describe the flow comprise equations for conservation of mass and momentum. The turbulence modeling was provided by a two-equation κ-ε model (for details see Zhang[3,9] and Zhang and Collins,[4] and a differential Reynolds stress model. The governing equations with the Reynolds stress turbulence closure model are

$$\frac{\partial \rho}{\partial t} + \nabla\cdot(\rho V) = 0 \tag{1}$$

$$\frac{\partial \rho V}{\partial t} + \nabla\cdot(\rho V \otimes V) = -\nabla p - \nabla\cdot(\rho \overline{v \otimes v}) \tag{2}$$

where v is the fluctuating velocity and the overbar indicates mean.

$\overline{v \otimes v}$ satisfies the equation

$$\frac{\partial \rho \overline{v \otimes v}}{\partial t} + \nabla\cdot(\rho \overline{v \otimes v} \otimes V) - \nabla\cdot\left[\rho C_S \frac{k}{\varepsilon} \overline{v \otimes v}(\nabla \overline{v \otimes v})^T\right] = P + \Phi - \frac{2}{3}\rho\varepsilon I \tag{3}$$

in which the stress production term P is given by

$$P = -\rho[\overline{v \otimes v}(\nabla V)^T + (\nabla V)\overline{v \otimes v}] \tag{4}$$

and Φ is the pressure-strain correction given as

$$\Phi = -\rho C_{1S}(\varepsilon/k)(\overline{v \otimes v} - \tfrac{2}{3}kI) - C_{2S}[P + \tfrac{2}{3}(\rho \overline{v \otimes v}\cdot\nabla V)I] \tag{5}$$

The governing equation for ε is given as

$$\frac{\partial \rho\varepsilon}{\partial t} + \nabla\cdot(\rho V\varepsilon) - \nabla\cdot\left(\rho C_\varepsilon \frac{k}{\varepsilon} \overline{v \otimes v}\nabla\varepsilon\right) = C_1 \frac{\varepsilon}{k}(-\rho \overline{v \otimes v}\cdot\nabla V) - C_2\rho\frac{\varepsilon^2}{k} \tag{6}$$

In the governing equations, C_S, C_{1S}, C_{2S}, C_ε, C_1, and C_2 are constants that are given values of 0.22, 1.8, 0.6, 0.16, 1.44, and 1.92, respectively. Descriptions of the wall reflection terms can be found in Clarke and Wilkes.[10]

IV. Numerical Approach

In the coordinate system (Fig. 1), the x axis is in the streamwise direction, the y axis the upward direction normal to the flat plate, and the z axis the lateral direction. The physical space in the flow is rectangular, its size varying according to the grid used. For the single jet study, a typical $50 \times 28 \times 42$ grid covering $-8D$ to $65D$, 0 to $11D$ and $-8D$ to $19D$ in the x, y, and z directions, respectively, was employed. The center of the jet exit was located at the origin of the coordinate system. In the lateral direction where the jet had a positive velocity component, the space covered was extended. The grid cell size increased gradually in the x and z directions. An exponential grid distribution was applied in the y direction and care was taken to locate at least 15 grid points in the boundary layer. For the co- and contrarotating jet study, the grid size varied from $60 \times 28 \times 16$ to $60 \times 28 \times 40$. A plain view of the grid near the jet exit is shown in Fig. 2. The grid cell size selection was tested in a previous single jet study[4] and was found to be adequate.

A fully developed velocity profile was used at the incoming boundary and was fixed. The boundary-layer profile was ob-

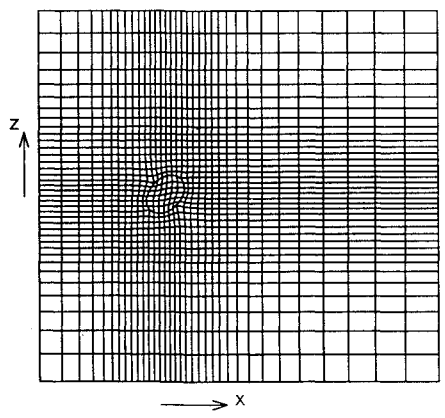

Fig. 2 Plane view of the grid near a single jet exit.

tained by calculating a two-dimensional turbulent boundary-layer development on a flat plate with an input velocity profile based on the one-seventh-law. Initial turbulence data were calculated using an eddy-viscosity model. On the downstream outer boundary, derivatives of the variables normal to the boundary were set to zero. Velocity components normal to the boundary were adjusted for mass conservation. On the flat plate, the no-slip condition was used. In the near-wall region, velocity was calculated using the classic linear–logarithmic wall-functions. On the jet exit plane, a "top hat" velocity profile was specified. The turbulent kinetic energy k and ε were approximated as

$$k_j = 0.002V_j^2 \quad \text{and} \quad \varepsilon_j = \frac{k_j^{1.5}}{0.3D}$$

The two side boundaries were set to periodic or symmetry conditions according to the co- and contrarotating jets selected.

The governing equations were solved using a finite volume solver, FLOW3D. All the terms in the governing equations were discretized in space using a second-order central differencing apart from the convective terms and the convection coefficients obtained by the Rhie–Chow interpolation formula. Hybrid differencing was used to treat the advective terms. The SIMPLEC algorithm alternative was employed in this work for the pressure-correction equation. The conjugate gradient algorithm was used for the pressure equation, while Stone's strongly implicit procedure (SIP) was used for the other equations. Underrelaxation was used as follows: factors were 0.7 for velocity, and 0.4 for k and ε. The calculation was performed on a SUN SPARC station2. CPU time and number of iterations varied according to the size of the problem. Convergence was judged to have been achieved when the mass residual was reduced by at least six orders of magnitude.

V. Results and Discussion

A. Single Inclined Jet

It is well known that when a jet exhausts normally into a crossflow, two contrarotating vortices are formed in the jet,

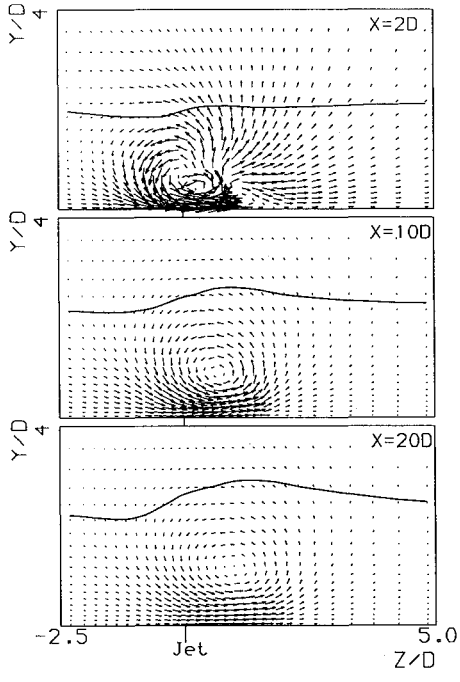

Fig. 3 Velocity vector plots a single vortex formation viewed in the upstream direction at α = 45 deg, θ = 90 deg, and λ_j = 0.7. Solid line indicates the edge of the boundary layer. Reynolds stress model.

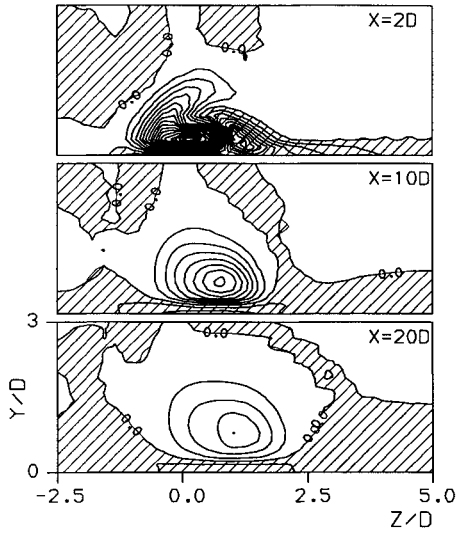

Fig. 4 $\bar{\Omega}_x\delta/V_\infty$ contours at α = 45 deg, θ = 90 deg, and λ_j = 0.7. Shadow area indicates the induced vorticity. Reynolds stress model.

as it is bent by the oncoming flow. The driving mechanism here is the momentum exchange between the jet and the crossflow. When an inclined jet is skewed to the crossflow a single streamwise vortex is eventually formed downstream instead of the two vortices. This phenomenon was first noticed by Wallis[5] using a θ = 90-deg skewed jet and surface pressure survey. In the computational analysis performed by Zhang,[3,9] it was suggested that the streamwise vortex development should be divided into two stages. The first is the formation of a single vortex through initial vorticity production, bending of the jet, and merging of vorticity areas of opposite signs. The second stage is the decaying of the streamwise vortex through turbulent mixing. At this stage of the vortex development the position of the vortex is important. At a small skew angle ($\theta \leq 30$ deg) or a small jet velocity ratio, the streamwise vortex is embedded deeply in the boundary layer and its strength is reduced rapidly. If the jet-skewed angle and the jet velocity ratio are selected to produce a streamwise vortex located near the edge of the boundary layer, the vortex would decay much more slowly.

In Figs. 3 and 4, the single streamwise vortex production by an inclined jet exhausting into a turbulent boundary layer is shown. The example shown is of the jet velocity ratio λ_j = 0.7. The velocity vector plot indicates that a single vortex is formed at a downstream distance of $X = 10D$. The single vortex is formed and continues to be located inside the boundary layer. Immediately downstream of the jet exit at $X = 2D$, a small contrarotating vortex is developed beside the main vortex. As the main vortex develops downstream it moves away from the wall and the jet exit. In the present study, the smallest skewed angle is 15 deg. At this skew angle a single vortex is still observed downstream. The vorticity distribution (Fig. 4) at $X = 2D$ shows clearly the contrarotating vortex beside the main vortex and the eventual formation of the single vortex. In the present analysis, the center of the jet is represented by the maximum vorticity position. In the vortex formation stage, the jet center defined in this way is different from that given by the maximum velocity.

An important parameter for quantifying the vortex is the circulation level Γ. It represents the overall strength of the vortex. In the study, θ and λ_j were varied to study their effects on the circulation level. Results are shown in Figs. 5 and 6. The variation of Γ with θ (Fig. 5) indicates that increasing the skew angle would result in an increase in the circulation level of the streamwise vortex. This effect is most pronounced between θ = 0 and 45 deg. Above θ = 45 deg the increase in Γ is small and above 60 deg the increase is negligible. In Fig.

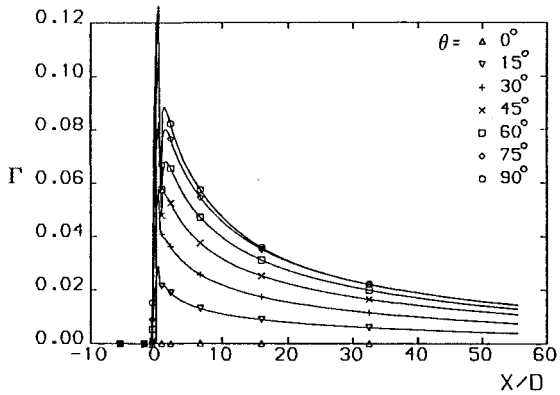

Fig. 5 Effect of θ on circulation level. α = 45 deg and λ_j = 1.0. k-ε model.

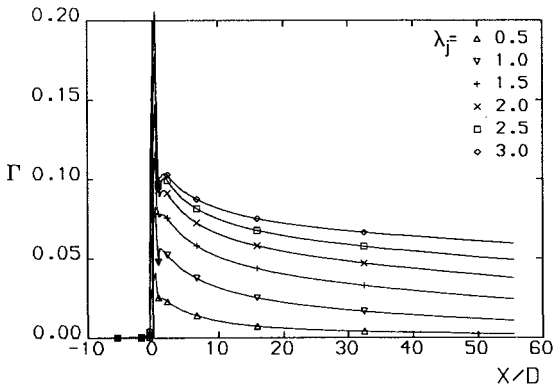

Fig. 6 Effect of λ_j on circulation level. α = 45 deg and θ = 45 deg. k-ε model.

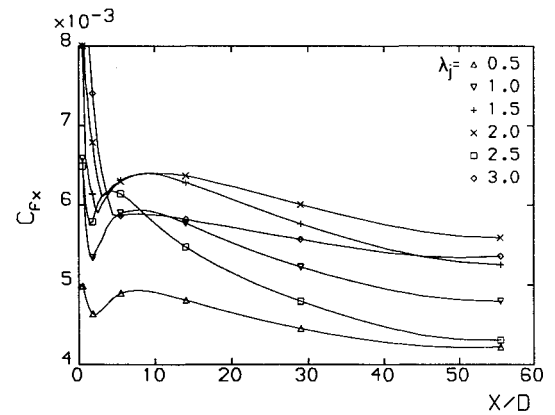

Fig. 7 Maximum C_{fx} downstream of the jet exit. α = 45 deg and θ = 45 deg. k-ε model.

6, the effect of λ_j is indicated by the continuous rise in Γ with λ_j. The rate of increase is slowed down above $\lambda_j \geq 1.5$. Although Γ is useful in quantifying the overall strength of the vortex, it gives little indication as to the stress field near the wall and the effectiveness of the vortex in preventing an impending likely separation. A much better parameter in judging the effectiveness of the streamwise vortex in terms of the separation control is the maximum C_{fx}, which is given in Fig. 7 at the various jet velocity ratios. High C_{fx} indicates that high kinetic energy fluid is brought to the near-wall region by the vortex. With it, the ability of the flow to resist the impending separation is enhanced. It follows that a high λ_j jet is not necessarily good for the separation control of a boundary layer, and for that matter, heat transfer enhancement. The jet will merely penetrate the boundary layer and the subsequently formed strong vortex is wasted. However, it could be effective for secondary flow control.

B. Comparison with Experimental Data

An attempt was made to compare the CFD prediction of the single jet generated vortex with the available experimental data. The purpose of the exercise was to validate the numerical model. The experiment chosen was that due to Compton and Johnston,[7] which was in fact the only wind-tunnel test giving a consistent set of data. In Compton and Johnston, the cross-plane velocity was presented in terms of velocity vector, positive circulation level, and maximum vorticity. As

Table 1 Positive circulation level

Single jet	X/D	Experiments	CFD	CFD[a]
λ_j = 0.7	20.47	0.010	0.0263	0.0186
α = 45 deg, θ = 90 deg	69.29	0.003	0.0128	0.0119
λ_j = 1.0	20.47	0.038	0.0494	0.0378
α = 45 deg, θ = 90 deg	69.29	0.023	0.0264	0.0247
λ_j = 1.3	20.47	0.079	0.0782	0.0630
α = 45 deg, θ = 90 deg	69.29	0.051	0.0434	0.0410
λ_j = 1.0	20.47	0.026	0.0397	0.0283
α = 45 deg, θ = 45 deg	69.29	0.019	0.0196	0.0179

[a]Γ calculated using same area as in Ref. 8.

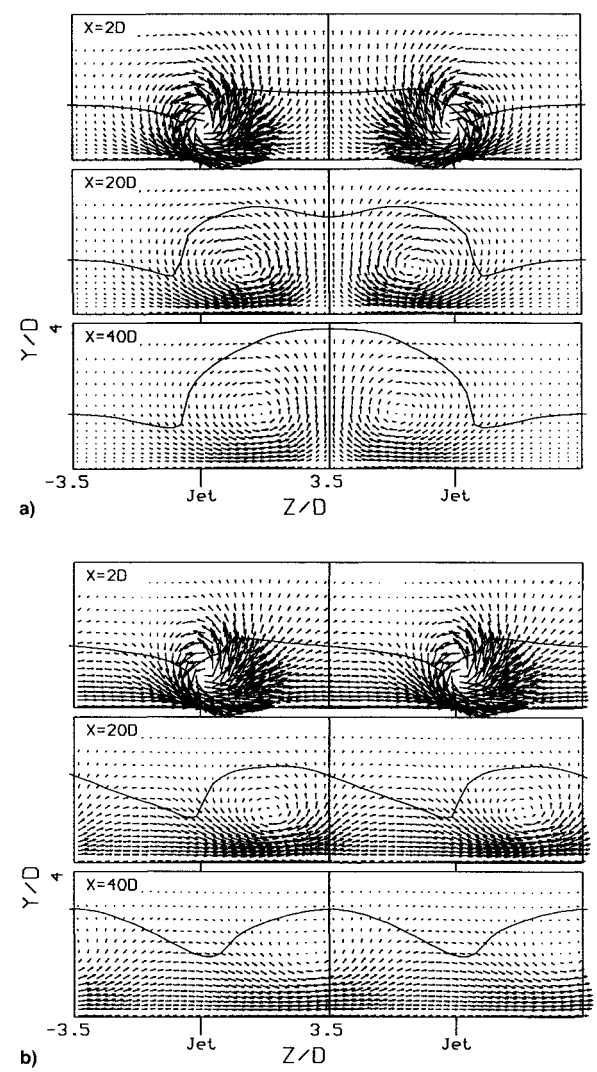

Fig. 8 Velocity vector plots of co- and contrarotating vortices viewed in the upstream direction. α = 45 deg, θ = 60 deg, λ_j = 1.5, and D_s = 7D. Solid line indicates the edge of boundary layer: a) contrarotating and b) corotating. Reynolds stress model.

Compton and Johnston used only a 0.5 × 0.5 cm measurement grid, the measurement accuracy of $\bar{\Omega}_x$ may not be high enough and only the positive cross-plane circulation level data were used here.

The results are listed in Table 1. The predicted positive Γ level is consistently higher than those given by Compton and Johnston. In Compton and Johnston, the closest measurement point to the flat plate was at a normal distance of 0.5 cm. Given that the boundary-layer thickness was about $\delta_{0.99}$ = 14 mm, their calculation excluded a substantial part of the near-wall region. The current predictions employing the same area as Compton and Johnston result in a much better agreement with the measured data, particularly at λ_j = 1.0 and 1.3. At λ_j = 0.7, the streamwise vortex is formed near the wall and that contributes to the discrepancy between the prediction and the measurement.

C. Co- and Contrarotating Jets

In engineering applications, a series of streamwise vortices are likely to be employed to suppress separation or to enhance heat transfer. It is important to study the co- and contrarotating jets in an oncoming flow. Based on the results of the single jet study, an α = 45 deg, θ = 60 deg, and λ_j = 1.5 jet was chosen for the co- and contrarotating jet study. The jet spacing was varied from D_s = 3D to 9D.

In Fig. 8, velocity vector plots of the co- and contrarotating jets at D_s = 7D are given, and in Fig. 9 the corresponding velocity contours are presented. The movement of the single vortex is seen to be quite similar to that generated by winglets.[1] Due to the jet efflux, the streamwise velocity near the center of the vortex is naturally higher than that generated by winglets. It is noticeable that the lateral movement of the vortex is restricted under the contrarotating arrangement, whereas under the corotating arrangement the vortices move in the lateral direction. In the case of the streamwise vortices produced by winglets under the contrarotating conditions, the interactions between the vortices and the image vortices all contribute to lift the vortices away from the wall.[1] This phenomenon introduces problems for the winglet-generated vortices as the winglets are usually fixed and the effectiveness of the control may be reduced downstream. For the vortices generated by the contrarotating jets, this phenomenon is not obvious under the present test conditions. It may well be that farther downstream the vortices will move away from the wall. This needs further study. Even if the vortices are to move away from the wall, the jets can be controlled to reduce this adverse effect. We can also see the superiority of the contrarotating jets as the ability of convecting high kinetic energy fluid to the near-wall region by one vortex is enhanced by the adjacent vortices.

Changes in C_{fx} are shown in contour form in Fig. 10. The advantages of using the contrarotating jets are indicated by the relatively large area of high C_{fx} to one side of the jet and the relatively small area of low C_{fx} to another side. The corotating jets produce a comparatively larger area of low C_{fx}. However, caution should be exercised in trying to interpret the current results. The contrarotating jets are likely to be effective under the current test conditions and within the limits imposed by the current length scales. It may well be that farther downstream the contrarotating vortices will move away from the wall and their effectiveness will be reduced. The current contrarotating jets, though, should be effective in

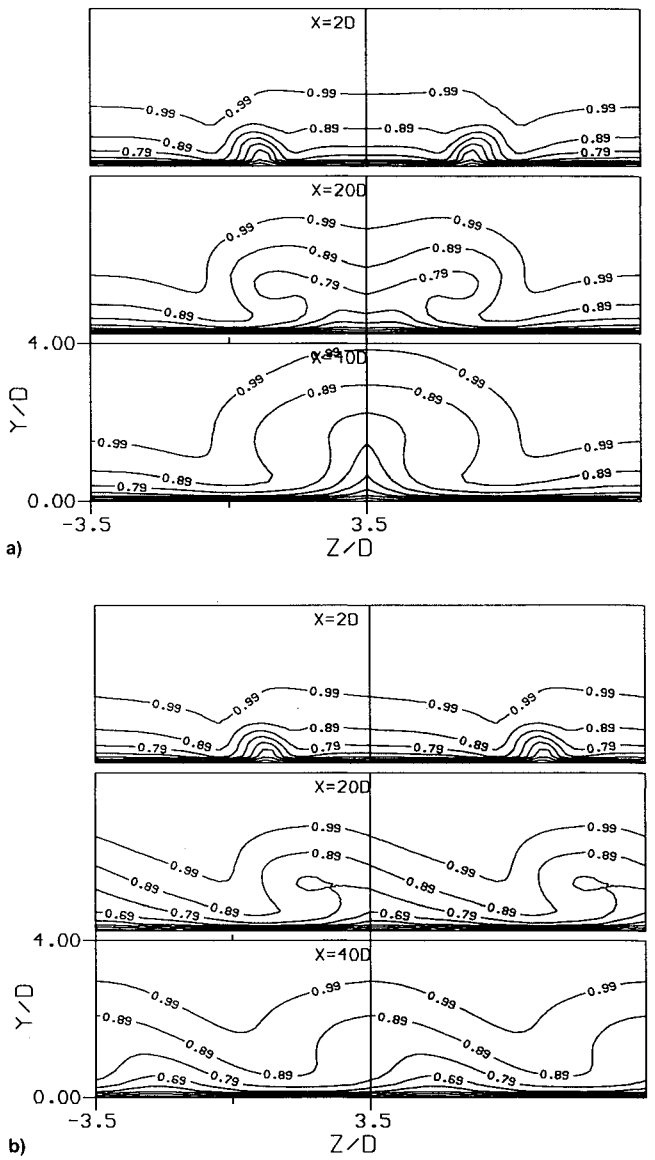

Fig. 9 (U/V_∞) contours of co- and contrarotating vortices viewed in the upstream direction. α = 45 deg, θ = 60 deg, λ_j = 1.5, and D_s = 3D: a) contrarotating and b) corotating. Reynolds stress model.

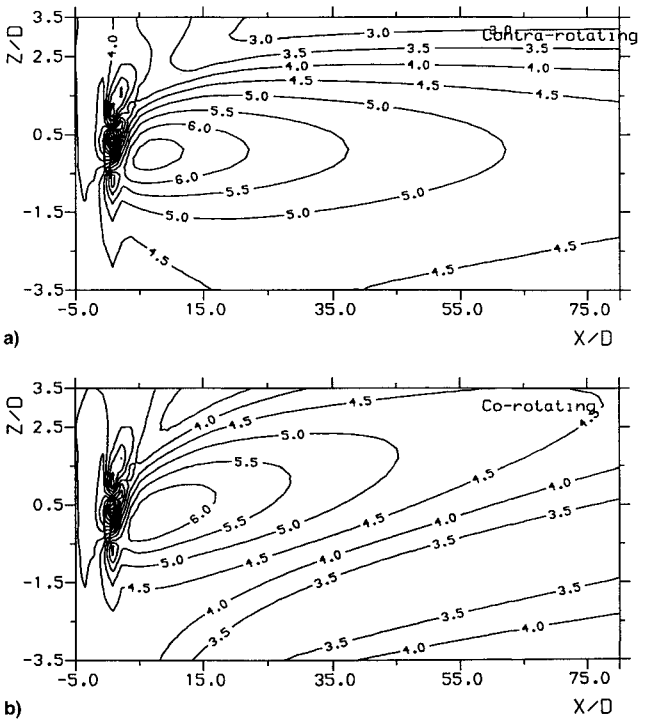

Fig. 10 C_{fx} on the flat plate at α = 45 deg, θ = 60 deg, λ_j = 1.5, and D_s = 3D: a) contrarotating and b) corotating. Reynolds stress model.

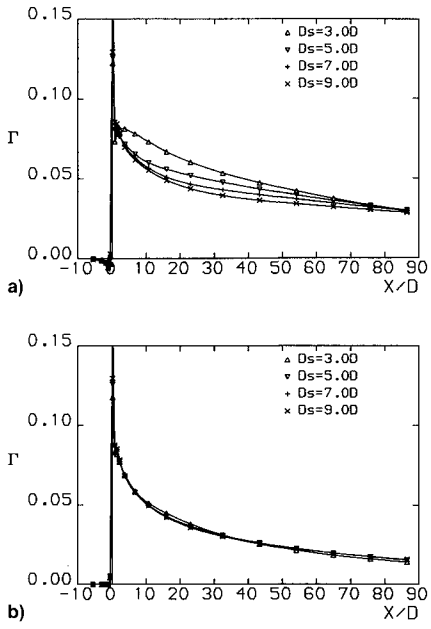

Fig. 11 Effect of jet spacing on Γ: a) contrarotating and b) corotating. Reynolds stress model.

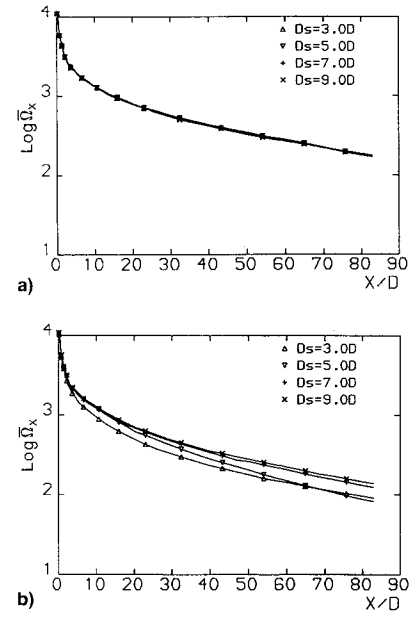

Fig. 12 Effect of jet spacing on maximum vorticity level: a) contrarotating and b) corotating. Reynolds stress model.

situations where the jets are located close to the separation line and for the purpose of active control.

The effect of the jet spacing on the overall circulation level is given in Fig. 11. The contrarotating jets are seen to produce higher Γ than the corotating jets. The jet spacing does not seem to affect Γ produced by the corotating jets. In the contrarotating setup, Γ drops initially as the jet spacing is increased. However, downstream of the jet exit the effect of the jet spacing on Γ is relatively small. The decaying process of the streamwise vortices is indicated by the value of the maximum vorticity level $\bar{\Omega}_x$. For the contrarotating jets the jet spacing does not influence the value of $\bar{\Omega}_x$, while for the corotating jets (Fig. 12) the vortices decay relatively quickly at the small jet spacings. As a result, there are no coherent vortices after a certain distance downstream. This is reflected by the lateral movement of the vortices shown in Fig. 13. For

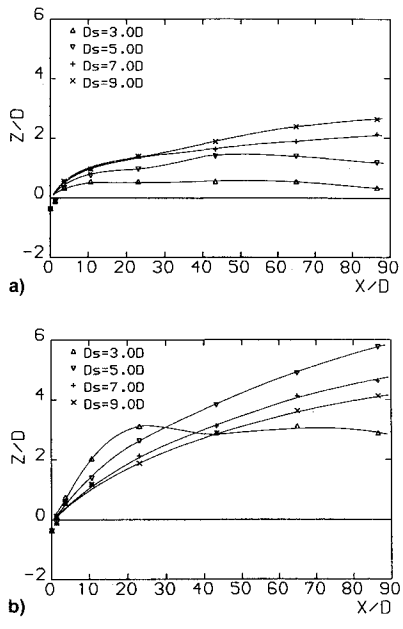

Fig. 13 Lateral movement of streamwise vortex: a) contrarotating and b) corotating. Reynolds stress model.

the contrarotating jets (Fig. 13a), the lateral movement of the vortices is restricted by the jet spacing. For the corotating jets at $D_s = 5D$, $7D$, and $9D$ the vortices move in the lateral direction according to the jet spacing. However, at $D_s = 3D$ the streamwise vortices are quickly diffused. After $X \geq 20D$ the coherent vortices are not maintained.

VI. Summary Remarks

In this study, a numerical analysis was performed on the streamwise vortices produced by a single jet and co- and contrarotating jets in a turbulent boundary layer. The mass-averaged Navier–Stokes equations were solved. Turbulence was modeled by a two-equation k-ε model and a differential stress model. The predicted positive cross-plane circulation levels were compared with a comparable experiment. When the same cross-plane area was used in the computation as that in the experiment, the agreement between the prediction and the experiment was found to be favorable. The true cross-plane circulation level was found to be considerably higher than that reported previously. The results indicated the importance of the near-wall region in defining the streamwise vortex effectiveness.

The study confirmed previous wind-tunnel observations that a single vortex was formed downstream of the jet exit. It also showed the formation of the vortex through the interaction of opposite vorticity areas. The effect of the jet skew angle was found to be relatively small between 60–90 deg, which agreed quite well with wind-tunnel observations. The study also suggested that jets with a high velocity ratio may not necessarily be effective for the boundary-layer separation control. The jets should be carefully controlled so that the vortices would be formed inside the boundary layer.

Contrarotating jets were seen to produce stronger streamwise vortices in the boundary layer than those by the corotating jets and should be effective when the jets were located near the separation line. The circulation level was found to decrease with the increase in the jet spacing. The maximum vorticity level of the individual vortex, though, was not affected by the jet spacing. Under the corotating arrangement, the total cross-plane circulation level was not affected by the jet spacing. However, the individual vortex decayed quickly compared to that in the contrarotating arrangement. A coherent vortex was not maintained after $X = 20D$ at a jet spacing of $D_s = 3D$.

Acknowledgment

The author wishes to thank the Nuffield Foundation for providing an award for the computational effort.

References

[1]Pearcey, H. H., "Shock Induced Separation and Its Prevention," *Boundary Layer & Flow Control*, Vol. 2, Pergamon, New York, 1961, pp. 1170–1344.

[2]Honami, S., Shizawa, T., and Uchiyama, A., "Behaviors of the Laterally Injected Jet in Film Cooling: Measurements of Surface Temperature and Velocity/Temperature Field Within the Jet," American Society of Mechanical Engineers International Gas Turbine and Aeroengine Congress and Exposition in Cologne, Germany, June 1992.

[3]Zhang, X., "Interaction Between a Turbulent Boundary Layer and Elliptic and Rectangular Jets," *Engineering Turbulence Modelling and Measurement*, edited by W. Rodi and F. Martelli, Elsevier, Amsterdam, 1993, pp. 251–260.

[4]Zhang, X., and Collins, M. W., "Flow and Heat Transfer in a Turbulent Boundary Layer Through Jets," *AIAA Journal*, Vol. 31, No. 9, 1993, pp. 1590–1599.

[5]Wallis, R. A., "The Use of Air Jets for Boundary Layer Control," Aerodynamics Research Labs., Aero. Note 110 (N-34736), Melbourne, Australia, Jan. 1952.

[6]Freestone, M. M., "Preliminary Tests at Low Speeds on the Vorticity Produced by Air-Jet Vortex Generators," Dept. of Aeronautics, City Univ., Research Memo Aero 85/01, London, Feb. 1985.

[7]Compton, D. A., and Johnston, J. P., "Streamwise Vortex Production by Pitched and Skewed Jets in a Turbulent Boundary Layer," *AIAA Journal*, Vol. 3, No. 3, 1992, pp. 640–647.

[8]Liandrat, J., Aupoix, B., and Cousteix, J., "Calculation of Longitudinal Vortices Imbedded in a Turbulent Boundary Layer," *Turbulent Shear Flows 5*, Springer–Verlag, Berlin, 1987, pp. 253–265.

[9]Zhang, X., "Streamwise Vortex Production in a Turbulent Flow through Wall Jets," *Numerical Methods in Laminar and Turbulent Flow*, edited by C. Taylor, Vol. VIII, Pt. 2, Pineridge, Swansea, Wales, UK, July 1993, pp. 875–886.

[10]Clarke, D. S., and Wilkes, N. S., "The Calculation of Turbulent Flows in Complex Geometries Using an Algebraic Stress Model," Harwell Lab., Rept. AERE R 13251, United Kingdom Energy Authority, Oxfordshire, England, UK, Aug. 1988.